V. The molecular geometry and the atomic labeling scheme for $[Mo([9]aneN_3)(CO)_3Br]^+$ are shown in Figure 1. The molybdenum atom is seven-coordinate; it is surrounded by three nitrogen atoms of the cyclic amine, three carbonyl groups, and one bromide ion. The geometry can be described as a 4:3 piano stool as has been found for diiododicarbonyltris(*tert*-butyl isocyanide)tungsten(II).[28] Features of the coordinated carbonyl and 1,4,7-triazacyclononane are unexceptional. The Mo–Br and Mo–C bond lengths agree well with values reported for related seven-coordinate compounds.[10]

The single crystals form with a water of crystallization that is bound via a relatively short hydrogen bond to one amine proton ($N7-O_w$ = 2.927 (3) Å). Carbonyl oxygens are not involved in hydrogen bonding. The oxygen atoms O4 and O3 of the perchlorate ion form rather long hydrogen bonds to O_w (3.056 (3) and 3.247 (3) Å, respectively).

Conclusion

In light of the presently available data, it can be concluded that there are strong analogies between the synthesis and chemistry of these 1,4,7-triazacyclononane complexes and those of the corresponding η^5-cyclopentadienyl species and the tris(1-pyrazolyl)borate complexes although the cyclopentadienide ion and the tris(1-pyrazolyl)borate anion are negatively charged. However, a great advantage of working with 1,4,7-triazacyclononane complexes is that the intermediate and the final products are usually more air, moisture, and light stable than their cyclopentadienyl counterparts.

Acknowledgment. Financial support of this research from the Fonds der Chemischen Industrie is gratefully acknowledged.

Registry No. $Cr(CO)_3L$, 88253-23-0; $Mo(CO)_3L$, 88253-24-1; $W(CO)_3L$, 88253-25-2; $[Mo_2O_5L_2](ClO_4)_2$, 88253-27-4; $[W_2O_5L_2](ClO_4)_2$, 88253-29-6; $[LMo(CO)_3Br]Br_3$, 88253-31-0; $[LMo(CO)_3Br]PF_6$, 88253-32-1; $[LMo(CO)_3Br]ClO_4 \cdot H_2O$, 88253-34-3; $[LMo(CO)_3I]ClO_4$, 88253-36-5; $[LW(CO)_3I]PF_6$, 88253-38-7; $[LMo(CO)_3H]BF_4$, 88253-40-1; $[LW(CO)_3H]BF_4$, 88253-42-3; $[LW(CO)_3H]ClO_4$, 88253-43-4; $[LCr(CO)_2(NO)]ClO_4$, 88253-45-6; $[LMo(CO)_2(NO)]ClO_4$, 88253-47-8; $[LW(CO)_2(NO)]BF_4$, 88253-49-0; $[LMo(NO)_2Br]Br$, 88253-50-3; $[LW(NO)_2Br]Br$, 88253-51-4; $[LMo(NO)_2H]ClO_4$, 88253-53-6; $[LMo(NO)(CN)_3]$, 88253-54-7; $Cr(CO)_6$, 13007-92-6; $Mo(CO)_6$, 13939-06-5; $W(CO)_6$, 14040-11-0; HNO_3, 7697-37-2; nitrous acid, 7782-77-6.

Supplementary Material Available: Listings of observed and calculated structure factor amplitudes, elemental analyses (Table I), and anisotropic temperature parameters (Table VI) (15 pages). Ordering information is given on any current masthead page.

(28) Dreyer, E. B.; Lam, C. T.; Lippard, S. J. *Inorg. Chem.* **1979**, *18*, 1904.

Contribution from the Chemistry Department and Materials and Molecular Research Division of Lawrence Berkeley Laboratory, University of California, Berkeley, California 94720

Bis(pentamethylcyclopentadienyl)ytterbium(II) as a Lewis Acid and Electron-Transfer Ligand. Preparation and Crystal Structures of $[Yb(Me_5C_5)_2(\mu\text{-}CO)_xMn(CO)_{5-x}]_y$ (x, y = 2; x = 3, y = ∞)

JAMES M. BONCELLA and RICHARD A. ANDERSEN*

Received June 2, 1983

The divalent ytterbium metallocene $(Me_5C_5)_2Yb(OEt_2)$ reacts with $Mn_2(CO)_{10}$ to give a compound of composition $(Me_5C_5)_2YbMn(CO)_5 \cdot {}^1/_4PhMe$, which was shown by an X-ray crystallographic study to be composed of a polymeric chain of $[(Me_5C_5)_2Yb(\mu\text{-}OC)_3Mn(CO)_2]$ units with dimeric units $[(Me_5C_5)_2Yb(\mu\text{-}OC)_2Mn(CO)_3]$ packed between the polymeric sheets. The toluene of solvation fills regularly spaced voids in the network of dimer and polymer sheets. The space group is $C2/m$ with a = 18.942 (5) Å, b = 32.592 (5) Å, c = 19.029 (5) Å, β = 109.92 (2)°, V = 11 045 (18) Å^3, and Z = 16. The contact-ion-pair complex results from $(Me_5C_5)_2Yb$ acting as an electron-transfer reagent, $(Me_5C_5)_2Yb \rightarrow (Me_5C_5)_2Yb^+ + 1e^-$, and as a Lewis acid by way of $Yb(\mu\text{-}OC)Mn$ interactions. The solution and solid-state infrared spectra are discussed relative to the alkali-metal analogues. The rhenium carbonyl $Re_2(CO)_{10}$ behaves similarly.

The concept of transition-metal carbonyl basicity, the ability of the lone pair of electrons on the oxygen atom to act as a Lewis base, is well-known.[1] In particular, group 3B compounds form acid–base complexes with the bridging carbonyl groups in, for example, $Cp_2Fe_2(\mu\text{-}CO)_2(CO)_2$ or $Cp_4Fe_4(\mu_3\text{-}CO)_4$.[2] The acid–base interaction leads to a reduction in the C–O stretching frequency; e.g., the bridging CO stretching frequency in $Cp_2Fe_2[(\mu\text{-}CO)AlEt_3]_2(CO)_2$ is lowered 113 cm^{-1} relative to that found in the acid-free complex.[2a,b] Carbonyl complexes whose solid-state structures do not contain bridging carbonyl groups and whose solution behavior is stereochemically rigid, e.g., $Mn_2(CO)_{10}$,[3] do not form complexes with aluminum compounds.[2b,d]

Early-transition-metal complexes also can act as Lewis acids toward metal carbonyls, giving complexes with M–CO–M′ interactions.[4] In these complexes the C–O stretching frequency also is lowered relative to that in the uncoordinated complex. In addition, it is generally observed that the M–C–O angle is essentially linear and the C–O–M′ angle is less than 180°. In particular, the Mo–C–O bond angle is 178.8 (4)° and the O–C–Ti angle is 144.3 (3)° in $CpMo(CO)_2[(\mu$-

* To whom correspondence should be addressed at the Chemistry Department.

(1) Shriver, D. F. *J. Organomet. Chem.* **1975**, *94*, 159; *Acc. Chem. Res.* **1970**, *3*, 231.
(2) (a) Nelson, N. J.; Kime, N. E.; Shriver, D. F. *J. Am. Chem. Soc.* **1969**, *91*, 5173. (b) Alich, A.; Nelson, N. J.; Strope, D.; Shriver, D. F. *Inorg. Chem.* **1972**, *11*, 2976. (c) Shriver, D. F.; Alich, A. *Ibid.* **1972**, *11*, 2984. (d) Kristoff, J. S.; Shriver, D. F. *Ibid.* **1974**, *13*, 499.
(3) (a) Dahl, L. F.; Rundle, R. E. *Acta Crystallogr.* **1963**, *16*, 419. (b) Martin, M.; Rees, B.; Mitschler, A. *Acta Crystallogr., Sect. B* **1982**, *B38*, 6. (c) Churchill, M. R.; Amoh, K. N.; Wasserman, H. J. *Inorg. Chem.* **1981**, *20*, 1609. (d) Todd, L. J.; Wilkinson, J. R. *J. Organomet. Chem.* **1974**, *77*, 1.
(4) (a) Schneider, M.; Weiss, E. *J. Organomet. Chem.* **1976**, *121*, 365. (b) Renault, P.; Tainturier, G.; Gautheron, B. *Ibid.* **1978**, *150*, 9. (c) Longato, B.; Norton, J. R.; Huffman, J. C.; Marsella, J. H.; Caulton, K. G. *J. Am. Chem. Soc.* **1981**, *103*, 209. (d) Hamilton, D. M.; Willis, W. S.; Stucky, G. D. *Ibid.* **1981**, *103*, 4255. (e) Barger, P. T.; Bercaw, J. E. *J. Organomet. Chem.* **1980**, *201*, C39. (f) Pasynskii, A. A.; Skripkin, Y. V.; Eremenko, I. L.; Kalinnikov, V. T.; Alexandrov, G. G.; Andrianov, V. G.; Struchkov, Yu. T. *Ibid.* **1979**, *165*, 49.

0020-1669/84/1323-0432$01.50/0

Table I. Infrared Spectra (ν(CO) in cm^{-1})

compd	medium	obsd bands	ref
$Mn(CO)_5Yb(Me_5C_5)_2$	THF	2030 w, 2010 m, 1934 s, 1903 s, 1770 s	this work
	Nujol	1965 s, 1937 sh, 1928 sh, 1882 m, 1840 s, 1775 s	
	cyclohexane	1984 m, 1962 s, 1955 s, 1945 m, 1778 m, 1762 s, 1750 m, 1723 m	
$LiMn(CO)_5$	THF	1895 s, 1861 s	16a
$NaMn(CO)_5$	THF	1902 s, 1897 s, 1875 s, 1862 s, 1829 m	16a
$KMn(CO)_5$	THF	1896 s, 1862 s, 1830 m	16b
$Mg(py)_4[Mn(CO)_5]_2$	PhMe	2031 w, 1928 s, 1904 s, 1721 s	16c
$Re(CO)_5Yb(Me_5C_5)_2$	Nujol	1982 sh, 1972 s, 1950 s, 1945 sh, 1785 sh, 1770 sh, 1750 br, s	this work
$Co(CO)_4Yb(Me_5C_5)_2(THF)$	THF	2025 m, 1935 s, 1885 w	7 and this work
	methylcyclohexane	2015 s, 1975 s, 1960 sh, 1945 s, 1930 s, 1825 sh, 1810 s, 1780 s, 1715 br, s	

$CO)Ti(Me_5C_5)_2Me]$.[4d] The bond angles in the titanium complex are remarkably similar to those found in $Cp_2W_2(CO)_4[(\mu\text{-}CO)_2AlMe_2]_2$, in which the W–C–O and C–O–Al angles are 172 (2) and 149 (2)°, respectively.[5] Thus, the Me_2Al^+ and $(Me_5C_5)_2TiMe^+$ groups have similar effects when these groups are bonded to the oxygen atom.

In the above examples, the oxidation state of the main-group or early transition metal does not change in the synthesis reaction; i.e., no formal electron transfer is observed. In a recent example, reaction of a divalent zirconium species with $Cp_2Fe_2(\mu\text{-}CO)_2(CO)_2$ gives the tetravalent zirconium complex $Cp_2Fe_2(\mu\text{-}CO)_2C_2O_2Zr(Me_5C_5)_2$.[6a] The two-electron-transfer process results in the formation of a carbon–carbon bond. The related reaction of $Cp_2Ti(CO)_2$ with $Cp_2Mo_2(CO)_4$ gives $Cp_2Ti(THF)(\mu\text{-}OC)Mo(CO)_2Cp$, the result of a one-electron-transfer process. We have shown that the divalent f-block-metal complex $Yb(Me_5C_5)_2(OEt_2)$ acts as a Lewis acid and a one-electron-transfer agent toward the metal–metal-bonded transition-metal carbonyl $Co_2(CO)_8$, giving $(CO)_3Co[(\mu\text{-}CO)Yb(Me_5C_5)_2(THF)]$.[7] The paramagnetism and bond lengths of this complex show that the ytterbium fragment is trivalent, the result of a one-electron-transfer process. Several bridging carbonyl, f-element complexes have been postulated on the basis of infrared data.[8] A plausible mechanism for the formation of the ytterbium–cobalt complex is to postulate an interaction between two Yb(II) atoms and the bridging carbonyl groups in $Co_2(CO)_8$, similar to that observed in $Co_2(CO)_6(\mu\text{-}CO)[(\mu\text{-}CO)AlBr_3]$,[2d] followed by an electron transfer into the lowest unoccupied molecular orbital of $Co_2(CO)_8$. Population of this orbital, which is metal–metal σ antibonding, causes cleavage of the metal–metal bond, giving $Co(CO)_4^-$ fragments.[9] This coordination, electron-transfer mechanism may be used to rationalize the formation of $(CO)_7Fe[(\mu_3\text{-}CO)_4Yb_2(Me_5C_5)_4]$[10] and the cleavage of binuclear transition-metal carbonyls by main-group metals.[11]

It was of interest to extend the reaction of $Yb(Me_5C_5)_2(OEt_2)$ with other metal–metal-bonded carbonyls to test the scope of the electron-transfer reaction. We were particularly interested in the reaction of $Mn_2(CO)_{10}$ since its LUMO is metal–metal antibonding[12] (similar to that found in $Co_2(CO)_8$), but it does not contain bridging carbonyl groups[3] (dissimilar to that found in $Co_2(CO)_8$). In addition, considerable effort has been spent on trying to reduce the bond order of coordinated carbon monoxide so that the C–O bond can be reduced by, for example, hydrogen to give synthetically useful oxygenated and other hydrocarbons.[13] The $Yb(Me_5C_5)_2$ group acts as a Lewis acid, polarizing the coordinated carbon monoxide molecule, and as a one-electron-transfer reagent, putting electron density into the lowest unoccupied molecular orbitals of carbon monoxide, which are C–O antibonding and metal–carbon bonding. These two processes will activate carbon monoxide and reduce its bond order. In this regard, this strategy might be a useful model for the "oxide mechanism" of Fischer–Tropsch chemistry.[14]

The diethyl ether complex of bis(pentamethylcyclopentadienyl)ytterbium reacts with decacarbonyldimanganese in toluene to give a blue complex of empirical composition $Mn(CO)_5Yb(Me_5C_5)_2 \cdot {}^1/_4PhMe$. Decacarbonyldirhenium behaves similarily, giving red $Re(CO)_5Yb(Me_5C_5)_2 \cdot {}^1/_4PhMe$. Both complexes react with methyl iodide to give $MeM(CO)_5$, where M is Mn or Re as shown by the infrared spectrum of a pentane extract of the reaction residue. Both complexes are paramagnetic on the basis of the width and shift of the Me_5C_5 resonances in the ^1H NMR spectra (see Experimental Section). The manganese complex follows Curie–Weiss behavior $[\chi_M = C_M(T-\theta)^{-1}]$ from 5 to 20 K with $C_M = 1.58 \pm 0.02$, $\theta = -0.69 \pm 0.18$ K, and $\mu_{eff} = 3.57 \pm 0.02\ \mu_B$ and from 80 to 300 K with $C_M = 2.225 \pm 0.005$, $\theta = -13.46 \pm 0.51$ K, and $\mu_{eff} = 4.237 \pm 0.005\ \mu_B$. The susceptibility values are indicative of trivalent ytterbium.[15] Thus, a one-electron transfer from $Yb(Me_5C_5)_2$ to the transition-metal fragment has occurred, similar to earlier observations.[7,10]

The infrared spectrum of the ytterbium–manganese complex in tetrahydrofuran is similar (five absorption bands) to that of $NaMn(CO)_5$ in THF (Table I). The infrared spectrum of $NaMn(CO)_5$ in THF has been interpreted as arising from either an equlibrium between solvent-separated and contact ion pairs or a single contact ion pair with local C_{2v} symmetry.[16] The five-line pattern observed for the ytterbium complex

(5) Conway, H. J.; Gainsford, G. J.; Schrieke, R. R.; Smith, J. D. *J. Chem. Soc., Dalton Trans.* **1975**, 2499.

(6) (a) Berry, D. H.; Bercaw, J. E.; Jircitano, A. J.; Mertes, K. B. *J. Am. Chem. Soc.* **1982**, *104*, 4712. (b) Merola, J. S.; Gentile, R. A.; Ansell, G. B.; Modrick, M. A.; Zentz, S. *Organometallics* **1982**, *1*, 1731.

(7) Tilley, T. D.; Andersen, R. A. *J. Chem. Soc., Chem. Commun.* **1981**, 985.

(8) (a) Marianelli, R. S.; Durney, M. T. *J. Organomet. Chem.* **1971**, *32*, C41. (b) Bennett, R. L.; Bruce, M. I.; Stone, F. G. A. *Ibid.* **1971**, *26*, 355. (c) Crease, A. E.; Legzdins, P. *J. Chem. Soc., Dalton Trans.* **1973**, 1501. (d) Onaka, S.; Furuichi, N. *J. Organomet. Chem.* **1979**, *173*, 77. (e) Onaka, S. *Inorg. Chem.* **1980**, *19*, 2131.

(9) Abrahamson, H. B.; Frazier, C. C.; Ginley, D. S.; Gray, H. B.; Lilienthal, J.; Tyler, D. R.; Wrighton, M. S. *Inorg. Chem.* **1977**, *16*, 1554.

(10) Tilley, T. D.; Andersen, R. A. *J. Am. Chem. Soc.* **1982**, *104*, 1772.

(11) (a) Hieber, W. *Angew. Chem., Int. Ed. Engl.* **1961**, *0*, 65; *Adv. Organomet. Chem.* **1970**, *8*, 1. (b) Abel, E. W.; Stone, F. G. A. *Q. Rev. Chem. Soc.* **1970**, *24*, 498. (c) Ellis, J. E.; Faltynek, *J. Chem. Soc., Chem. Commun.* **1975**, 966; *J. Am. Chem. Soc.* **1977**, *99*, 1801. (d) Behrens, H.; Ruyter, E.; Wakamatsu, W. *Z. Anorg. Allg. Chem.* **1967**, *349*, 241. (e) McVicker, G. B. *Inorg. Chem.* **1975**, *14*, 2087. (f) Ulmer, S. W.; Skarstad, P. M.; Burlitch, J. M.; Hughes, R. E. *J. Am. Chem. Soc.* **1973**, *95*, 4469. (g) Burlitch, J. M. *Chem. Commun.* **1968**, 887; *Inorg. Chem.* **1970**, *9*, 563. (h) Hsieh, A. T. T.; Mays, M. J. *J. Chem. Soc. A* **1971**, 2648; *J. Chem. Soc., Dalton Trans.* **1972**, 516. (i) Haupt, H. J.; Wolfes, W.; Preut, H. *Inorg. Chem.* **1976**, *15*, 2920.

(12) Levenson, R. A.; Gray, H. B.; Ceasar, G. P. *J. Am. Chem. Soc.* **1970**, *92*, 3653.

(13) (a) Muetterties, E. L.; Stein, J. *Chem. Rev.* **1979**, *79*, 479. (b) Rofer-Depoorter, C. K. *Ibid.* **1981**, *81*, 447. (c) Herrmann, W. A. *Angew. Chem., Int. Ed. Engl.* **1982**, *21*, 117.

(14) Sapienza, R. S.; Sansone, M. J.; Spaulding, L. D.; Lynch, J. F. *Fundam. Res. Homogeneous Catal. [Proc. Int. Workshop]* **1979**, *3*, 179.

(15) (a) Tilley, T. D.; Zalkin, A.; Andersen, R. A.; Templeton, D. H. *Inorg. Chem.* **1981**, *20*, 551. (b) Tilley, T. D.; Andersen, R. A.; Zalkin, A.; Templeton, D. H. *Ibid.* **1982**, *21*, 2644.

(16) (a) Darensbourg, M. Y.; Darensbourg, D. J.; Burns, D.; Drew, D. A. *J. Am. Chem. Soc.* **1976**, *98*, 3127. (b) Ellis, J. E.; Flom, E. A. *J. Organomet. Chem.* **1975**, *99*, 263. (c) Ulmer, S. W.; Skarstad, P. M.; Burlitch, J. M.; Hughes, R. E. *J. Am. Chem. Soc.* **1973**, *95*, 4469.

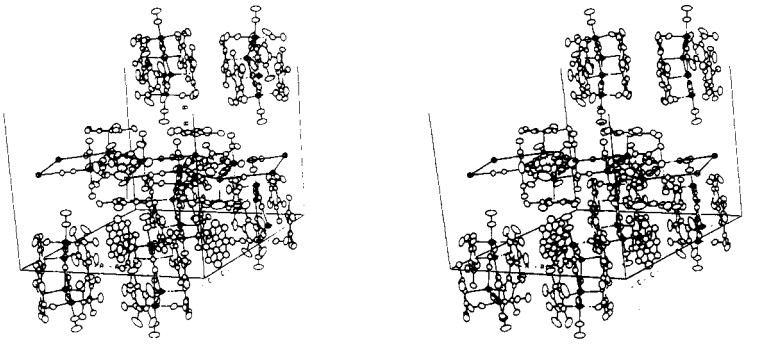

Figure 1. Stereopair view oblique to the *ac* plane.

suggests a similar explanation. We cannot distinguish between these two explanations, though some support for the existence of a contact ion pair of C_s symmetry is found by examining the infrared spectrum of the related complex $(Me_5C_5)_2Yb(\mu\text{-}OC)Co(CO)_3(THF)$ in tetrahydrofuran (Table I). In the solid state this molecule is a contact ion pair in which the ytterbium atom is bonded to a carbonyl oxygen atom and a tetrahydrofuran molecule.[7] The infrared spectrum of this complex in tetrahydrofuran has four absorptions expected for a structure of local C_s symmetry. The infrared spectrum of the ytterbium–manganese complex in tetrahydrofuran is consistent with a solution structure analogous to that of the ytterbium–cobalt complex, i.e., a contact ion pair in which the ytterbium atom is coordinated to a carbonyl oxygen atom and a tetrahydrofuran molecule.

The infrared spectra of the ytterbium–manganese complex in solid state or in cyclohexane solution are much more complex than in tetrahydrofuran, suggesting that other species are present in a noncoordinating solvent or in the solid. This is confirmed by the crystal and molecular structure of the complex.

Figure 1 shows a stereopair view of a portion of the unit cell oblique to the *ac* plane. Only half of the *b* axis is shown. A full layer of the structure of 0 and 0.25 in *y* is shown. A portion of the $y = 0.5$ layer shows how these layers pack in the unit cell.

Inspection of Figure 1 shows that the structure consists of layers of infinite, planar, polymeric sheets of the stoichiometry $\{[(Me_5C_5)_2Yb][Mn(CO)_5]\}_\infty$. Dimeric molecules of the formula $\{[(Me_5C_5)_2Yb][Mn(CO)_5]_2\}$ are packed between polymeric sheets. The solvating toluene molecules fill regularly spaced voids in the network of dimers and polymer sheets.

Close inspection of the polymeric sheet reveals that it consists of essentially trigonal-bipyramidal $Mn(CO)_5$ groups that are each coordinated to three different $(Me_5C_5)_2Yb$ groups through their equatorial carbonyls. Each $(Me_5C_5)_2Yb$ cation is in turn coordinated only to the equatorial carbonyls of the $Mn(CO)_5$ units, and all the Mn and Yb atoms in the polymer are essentially coplanar. The largest deviation of a metal atom from the least-squares plane through them is 0.065 Å by Yb1.

The dimeric $Mn(CO)_5Yb(Me_5C_5)_2$ units are disposed about the mirror plane at $y = 0$ such that two ytterbium atoms lie in the mirror plane and the manganese atoms lie above and below the mirror plane. In addition, all four Me_5C_5 rings in the dimer are bisected by the mirror plane and normal to it. The dimers pack in the *ac* plane at $y = 0$ with the disordered toluene molecule filling the voids such that the overall composition of the crystal is $[Mn(CO)_5Yb(Me_5C_5)_2]_4[PhMe]$. The crystal structure, then, consists of alternate planar, polymeric sheets normal to *b* with dimers at 0, $^1/_2$, 1, etc. and the polymer at $^1/_4$, $^3/_4$, etc.

The very complex, though regular, crystal structure rationalizes in a general, though not in an analytic, fashion with the large number of C–O stretching frequencies observed in the spectrum of the solid. It also offers a rationalization for the complexity of the infrared spectrum in the ν(CO) region in nonpolar solvents. The presence of oligomers and C_{2h} dimers, or dimers that do not have rigorous C_{2h} point symmetry in solution, is consistent with the observed spectra. The formation of dimers or other higher oligomers by the compound $[(Me_5C_5)_2Yb][Co(CO)_4]\cdot THF$ is consistent with the complexity of its ν(CO) IR spectrum in noncoordinating solvents (see Table I).

In the discussion that follows, we will describe the discrete dimeric and polymeric units with respect to their individual

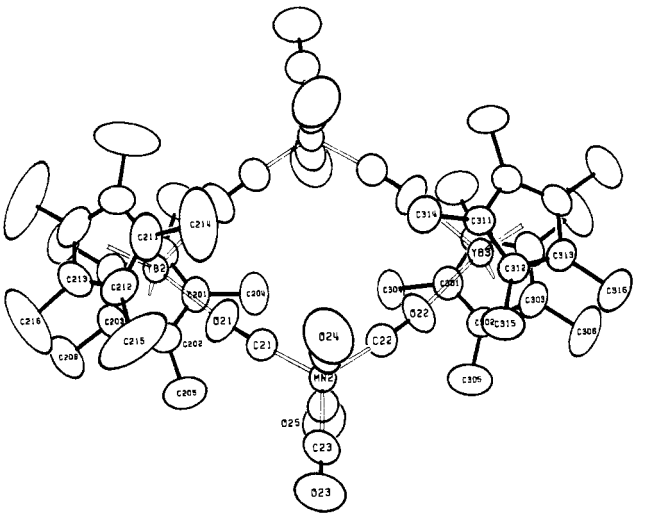

Figure 2. ORTEP view of the dimeric molecule.

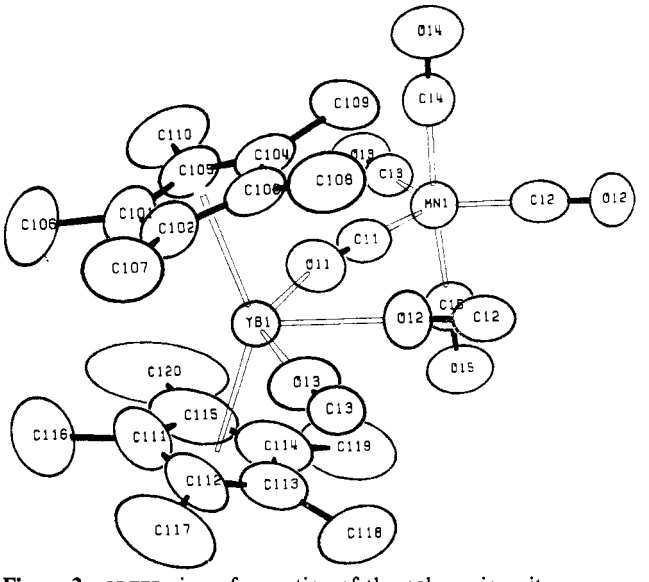

Figure 3. ORTEP view of a portion of the polymeric unit.

Table II. Positional Parameters

atom	x	y	z	atom	x	y	z
Yb1	0.05730 (2)	0.25203 (1)	0.28381 (2)	C311	0.5105 (4)	0.0000 (0)	0.1682 (4)
Yb2	0.10509 (2)	0.00000 (0)	−0.19709 (2)	C312	0.5250 (3)	0.0349 (2)	0.2142 (3)
Yb3	0.40884 (2)	0.00000 (0)	0.22843 (2)	C313	0.5481 (3)	0.0216 (2)	0.2893 (3)
Mn1	0.35154 (6)	0.25059 (3)	0.42052 (6)	C314	0.4887 (6)	0.0000 (0)	0.0835 (5)
Mn2	0.27408 (6)	0.09670 (3)	0.00619 (5)	C315	0.5231 (4)	0.0796 (2)	0.1890 (4)
O11	0.1919 (3)	0.2511 (1)	0.3235 (3)	C316	0.5841 (4)	0.0488 (3)	0.3594 (4)
O12	0.3902 (3)	0.2517 (1)	0.5853 (3)	C102	−0.0224 (4)	0.3165 (2)	0.2306 (4)
O13	0.4594 (3)	0.2498 (1)	0.3385 (3)	C103	0.0263 (4)	0.3273 (2)	0.3027 (4)
O14	0.3609 (3)	0.3417 (2)	0.4285 (3)	C104	0.0994 (4)	0.3283 (2)	0.3026 (4)
O15	0.3513 (3)	0.1600 (2)	0.4306 (3)	C105	0.0970 (4)	0.3181 (2)	0.2314 (4)
O21	0.1790 (2)	0.0472 (2)	−0.1183 (2)	C106	−0.0081 (6)	0.3088 (3)	0.0997 (4)
O22	0.3551 (2)	0.0475 (2)	0.1386 (2)	C107	−0.1087 (4)	0.3163 (3)	0.2028 (5)
O23	0.2790 (5)	0.1869 (2)	−0.0103 (4)	C108	0.0036 (5)	0.3401 (3)	0.3706 (4)
O24	0.4040 (3)	0.0903 (2)	−0.0464 (3)	C109	0.1687 (5)	0.3420 (2)	0.3695 (5)
O25	0.1500 (3)	0.1079 (2)	0.0668 (3)	C110	0.1650 (5)	0.3200 (3)	0.2014 (5)
C11	0.2543 (4)	0.2513 (2)	0.3624 (4)	C111	0.0048 (6)	0.1994 (3)	0.1751 (4)
C12	0.3749 (4)	0.2514 (2)	0.5189 (4)	C112	−0.0276 (5)	0.1887 (3)	0.2277 (4)
C13	0.4175 (4)	0.2499 (2)	0.3710 (4)	C113	0.0275 (5)	0.1753 (2)	0.2886 (4)
C14	0.3564 (4)	0.3065 (2)	0.4240 (4)	C114	0.0951 (4)	0.1767 (2)	0.2808 (5)
C15	0.3515 (4)	0.1950 (2)	0.4258 (4)	C115	0.0844 (5)	0.1915 (3)	0.2095 (5)
C21	0.2174 (3)	0.0683 (2)	−0.0691 (3)	C116	−0.0440 (11)	0.2086 (4)	0.0915 (6)
C22	0.3238 (3)	0.0685 (2)	0.0868 (3)	C117	−0.1148 (6)	0.1871 (4)	0.2117 (8)
C23	0.2781 (5)	0.1522 (2)	−0.0039 (5)	C118	0.0175 (6)	0.1577 (3)	0.3622 (5)
C24	0.3541 (4)	0.0929 (2)	−0.0273 (4)	C119	0.1672 (6)	0.1598 (3)	0.3383 (8)
C25	0.1968 (4)	0.1042 (2)	0.0426 (4)	C120	0.1410 (7)	0.1974 (4)	0.1671 (7)
C101	0.0220 (4)	0.3113 (2)	0.1860 (4)	C201	0.0377 (5)	0.0000 (0)	−0.1017 (4)
C212	0.1677 (4)	0.0344 (2)	−0.2820 (3)	C202	0.0109 (3)	0.0355 (2)	−0.1462 (3)
C213	0.1000 (4)	0.0207 (2)	−0.3286 (3)	C203	−0.0332 (3)	0.0213 (2)	−0.2199 (3)
C214	0.2913 (6)	0.0000 (0)	−0.2002 (7)	C204	0.0862 (6)	0.0000 (0)	−0.0187 (5)
C215	0.1919 (7)	0.0791 (3)	−0.2724 (5)	C205	0.0199 (4)	0.0800 (3)	−0.1188 (5)
C216	0.0375 (6)	0.0482 (4)	−0.3835 (5)	C206	−0.0823 (4)	0.0482 (3)	−0.2819 (4)
C301	0.2777 (5)	0.0000 (0)	0.2418 (4)	C211	0.2107 (5)	0.0000 (0)	−0.2525 (5)
C302	0.3151 (3)	0.0349 (2)	0.2812 (3)	C1	0.2198 (6)	0.0668 (4)	0.4919 (6)
C303	0.3750 (3)	0.0210 (2)	0.3443 (3)	C2	0.2213 (9)	0.0198 (5)	0.4886 (8)
C304	0.2088 (5)	0.0000 (0)	0.1714 (5)	C3	0.1959 (7)	0.0000 (0)	0.5400 (7)
C305	0.2918 (4)	0.0798 (2)	0.2633 (4)	C4	0.1974 (10)	0.0446 (6)	0.5377 (9)
C306	0.4224 (5)	0.0491 (3)	0.4089 (4)	C5	0.2434 (9)	0.0453 (5)	0.4458 (8)
				C6	0.2469 (7)	0.0000 (0)	0.4408 (6)

Table III. Selected Bond Lengths (Å)

Yb1-O11	2.401 (5)	Mn1-C11	1.796 (7)
Yb1-O12	2.349 (4)	Mn1-C12	1.771 (8)
Yb1-O13	2.417 (5)	Mn1-C13	1.805 (8)
Yb1-C101	2.607 (6)	Mn1-C14	1.825 (7)
Yb1-C102	2.584 (6)	Mn1-C15	1.814 (7)
Yb1-C103	2.578 (6)	Mn1-O11	2.957 (5)
Yb1-C104	2.599 (6)	Mn1-O12	2.968 (5)
Yb1-C105	2.590 (6)	Mn1-O13	2.963 (5)
Yb1-CP11[a]	2.304	Mn1-O14	2.974 (5)
Yb1-C111	2.610 (7)	Mn1-O15	2.959 (5)
Yb1-C112	2.612 (7)	Mn2-C21	1.735 (6)
Yb1-C113	2.571 (7)	Mn2-C22	1.761 (6)
Yb1-C114	2.564 (7)	Mn2-C23	1.823 (8)
Yb1-C115	2.577 (7)	Mn2-C24	1.839 (8)
Yb1-CP12[a]	2.305	Mn2-C25	1.838 (8)
Yb2-O21	2.268 (4)	Mn2-O21	2.924 (4)
Yb2-C201	2.551 (7)	Mn2-O22	2.940 (4)
Yb2-C202	2.576 (5)	Mn2-O23	2.962 (6)
Yb2-C203	2.599 (5)	Mn2-O24	2.964 (6)
Yb2-CP21[b]	2.279	Mn2-O26	2.972 (6)
Yb2-C211	2.560 (9)	C11-O11	1.161 (7)
Yb2-C212	2.565 (6)	C12-O12	1.197 (8)
Yb2-C213	2.563 (5)	C13-O13	1.159 (8)
Yb2-CP22[b]	2.283	C14-O14	1.149 (7)
Yb3-O22	2.273 (4)	C15-O15	1.145 (7)
Yb3-C301	2.582 (8)	C21-O21	1.190 (6)
Yb3-C302	2.582 (5)	C22-O22	1.181 (6)
Yb3-C303	2.590 (5)	C23-O23	1.139 (8)
Yb3-CP31[b]	2.292	C24-O24	1.125 (8)
Yb3-C311	2.554 (7)	C25-O25	1.135 (8)
Yb3-C312	2.572 (5)		
Yb3-C313	2.591 (5)		
Yb3-CP32[b]	2.280		

[a] Centroid of the five carbons above. [b] Centroid of cyclopentadiene ring generated by the three carbons above.

Table IV. Selected Bond Angles (deg)

Mn1-C11-O11	178.2 (5)	C21-Mn2-C23	118.6 (3)
Mn1-C12-O12	179.4 (6)	C21-Mn2-C24	91.7 (3)
Mn1-C13-O13	179.1 (5)	C21-Mn2-C25	91.9 (3)
Mn1-C14-O14	177.9 (6)	C22-Mn2-C23	125.5 (3)
Mn1-C15-O15	178.6 (6)	C22-Mn2-C24	90.4 (3)
Mn2-C21-O21	176.7 (5)	C22-Mn2-C25	90.0 (3)
Mn2-C22-O22	175.9 (5)	C23-Mn2-C24	87.8 (4)
Mn2-C23-O23	178.6 (9)	C23-Mn2-C25	88.5 (4)
Mn2-C24-O24	178.6 (6)	C24-Mn2-C25	175.7 (3)
Mn2-C25-O25	177.8 (7)	O11-Yb1-O12	69.20 (18)
Yb1-O11-C11	160.4 (5)	O11-Yb1-O13	138.85 (17)
Yb1-O12-C12	169.1 (5)	O12-Yb1-O13	69.65 (18)
Yb1-O13-C13	173.7 (5)	CP11[a]-Yb1-O11	95.8
Yb2-O21-C21	170.6 (4)	CP11-Yb1-O12	107.9
Yb3-O22-C22	172.5 (4)	CP11-Yb1-O13	96.7
C11-Mn1-C12	119.0 (3)	CP12-Yb1-O11	97.5
C11-Mn1-C13	115.2 (3)	CP12-Yb1-O12	108.7
C11-Mn1-C14	92.2 (3)	CP12-Yb1-O13	95.4
C11-Mn1-C15	91.5 (3)	CP11-Yb1-CP12	143.4
C12-Mn1-C13	125.8 (3)	O21-Yb2-O21	85.41 (24)
C12-Mn1-C14	87.4 (3)	O21-Yb2-CP21	103.5
C12-Mn1-C15	87.8 (3)	O21-Yb2-CP22	102.9
C13-Mn1-C14	89.8 (3)	CP21-Yb2-CP22	143.8
C13-Mn1-C15	91.7 (3)	O22-Yb3-O22	85.85 (22)
C14-Mn1-C15	174.9 (3)	O22-Yb3-CP31	103.1
C21-Mn2-C22	116.0 (3)	O22-Yb3-CP32	103.2
		CP31-Yb3-CP32	143.8

[a] CP11, CP12, etc. are the centroids of the ring carbons of the pentamethylcyclopentadiene ligands.

stereochemistry. An ORTEP view of the dimeric units is shown in Figure 2, and a portion of the polymeric unit in Figure 3. Positional parameters are shown in Table II, and some bond lengths and bond angles in Tables III and IV, respectively.

Table V. Crystal Data (25 °C) for $Mn(CO)_5Yb(Me_5C_5)_2 \cdot {}^1/_4PhMe$

space group	$C2/m$
a, Å	18.942 (5)
b, Å	32.591 (5)
c, Å	19.029 (5)
β, deg	109.92 (2)
V, Å^3	11045 (8)
Z	16
fw	661.27
d(calcd), g cm^{-3}	1.591
μ(calcd), cm^{-1}	38.27
size, mm	0.18 × 0.19 × 0.42
reflcns, collected	14 401
reflcns, unique	7442
reflcns, $F_o^2 > 3\sigma(F_o^2)$	5487
R, %	2.79
R_w, %	3.91
variables	614
GOF	1.578
monochromator	highly oriented graphite
radiation	Mo Kα (λ = 0.710 73 Å)
scan range, type	$3° \leq \theta \leq 45°$, θ–2θ
scan speed, deg min^{-1}	0.575–6.7
scan width, deg	$\Delta\theta = 0.45 + 0.347 \tan\theta$

Crystal data are shown in Table V. As alluded to earlier, the Mn_2Yb_2 unit is not planar. The angle between the normals of the two planes defined by Yb2–Yb3–Mn2 and Yb2–Yb3–Mn2′ is 15.2°. The plane defined by Yb2–Yb3–Mn2′ is essentially coplanar with the equatorial carbonyl ligands on Mn2. The distortion of the dimeric unit from planarity also may be described by reference to the Mn2–Yb2–Mn2′ and Mn2–Yb3–Mn2′ planes, which form a dihedral angle of 11.8°. In addition, the dihedral angles formed by extension of the centroids of the Me_5C_5 rings CP21–CP31 and CP22–CP32 (see Table III for the definition of these symbols) are 17.5 and 51.6°, respectively.

The average ytterbium–carbon length in the dimer is 2.574 ± 0.013 Å, and the average ytterbium–centroid distance is 2.281 ± 0.002 Å. The centroid–Yb–centroid angle is 143.8°. These bond lengths are in the range found for other Yb(III) complexes in eight-coordination[7,10,15c] and significantly shorter (0.17 Å) than those found for a Yb(II) ion in eight-coordination.[17] The average ytterbium–oxygen bond length is 2.271 ± 0.002 Å, and the average O–Yb–O angle is 85.63 ± 0.22°. These bond parameters in the dimer are very similar to those found in the polymer, even though the coordination number of ytterbium is 9 in the latter, the only difference being the ytterbium–oxygen bond lengths. In the polymer the average ytterbium–carbon bond length is 2.589 ± 0.015 Å, the ytterbium–centroid distance is 2.304 Å, the ytterbium–oxygen bond length is 2.389 ± 0.027 Å, and the average O–Yb–O angle is 69.43 ± 0.006°.

The coordination geometries of the pentacarbonylmanganate fragment in the dimer and polymer are very similar, both being related to a trigonal bipyramid, as found in $[Ni(phen)_3][Mn(CO)_5]_2$.[18a] The most important feature, perhaps, of the ytterbium–manganese complex is the carbonyl groups that bridge the ytterbium and manganese atoms. In the dimer two equatorial carbonyl groups are bonded to two different ytterbium atoms, and in the polymer all three equatorial carbonyl groups are bonded to three ytterbium atoms. In the dimer the average Yb–O–C and Mn–C–O angles are 171.6 ± 0.9 and 176.3 ± 0.4°, respectively. In the polymer, these average angles are 167.7 ± 0.5 and 178.9 ± 0.3°.

The average terminal manganese–carbon bond lengths in the dimer and polymer are 1.833 ± 0.007 and 1.820 ± 0.005 Å, respectively, whereas the bridging manganese–carbon distances are 1.748 ± 0.013 and 1.791 ± 0.013 Å, respectively. These distances may be compared with the average terminal manganese to carbon (equatorial) distance in $Mn_2(CO)_{10}$ of 1.856 ± 0.005 Å[3b,c] and in a number of anionic $Mn(CO)_5$ fragments that range from 1.78 to 1.82 Å.[18] In the ytterbium–manganese complex the shortened bridging manganese–carbon distance, relative to the terminal distance, is consistent with the view that electron transfer into a neutral $Mn(CO)_5$ fragment puts electron density into molecular orbitals that are C–O antibonding and Mn–C bonding. The carbon–oxygen bond lengths are also consistent with this view (Table III) though these distances are not determined with high accuracy. The variations of the manganese–carbon and carbon–oxygen bond lengths suggest that the resonance structure I and II are

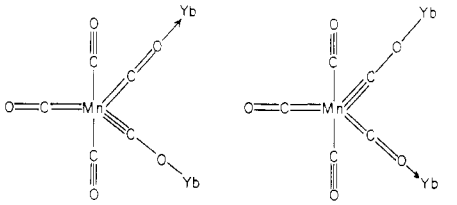

I II

important in the bonding in the contact ion pair. Further, structure I and II emphasize that contact-ion-pair formation tends to localize electron density into the manganese–carbon bonds that are part of the Mn–CO–Yb interaction.

Experimental Section

All operations were carried out under nitrogen. Microanalyses were performed by the microanalytical laboratory of this department. The ^1H nuclear magnetic resonance spectra were measured at 89.56 MHz on a JEOL FX90-Q instrument at 25 °C in benzene-d_6 (δ 7.15) and are expressed in δ values ($\delta(Me_4Si) = 0$). Infrared spectra were recorded on a Perkin-Elmer 597 instrument; solid spectra were measured as Nujol mulls, and solution spectra were measured in matched NaCl cells, with spacings of either 0.5 or 0.05 mm. The magnetic susceptibility measurements were made on an SHE Corp. Model 905 Squid magnetometer. The sample containers were made from an alloy of aluminum with 3% silicon purchased from Varian. The sample containers were held together with a 2-cm piece of 0.027-mm copper wire and sealed with silicon stopcock grease. The variation in the susceptibility of the container due to differing amounts of grease was less than 3%. The containers were designed by Dr. E. Gamp, and the design is available from the authors. The sample was loaded in a drybox, transported to the magnetometer in a Schlenk tube, and suspended in the sample chamber by a piece of cotton thread attached to the copper wire. Sample measurements were made automatically at the following temperatures and magnetic field strengths: At 5-kG magnetic field strength over a temperature range of 5–15 K, a datum was measured every 2.5 K, at 15–50 K every 5 K, and at 50–300 K every 10 K. At 40-kG magnetic field strength over a temperature range of 5–30 K, a datum was measured every 5 K, at 30–100 K every 10 K, and at 100–300 K every 20 K. All samples were corrected for container magnetism and compound diamagnetism by using Pascal constants. Temperature-independent paramagnetism was taken to be zero for ytterbium(III). The molar susceptibility was calculated, and the molar susceptibility was plotted as a function of the absolute temperature. A least-squares fit to the line, using a program written by Dr. E. Gamp, gave C_M where $\chi_M = C_M(T - \theta)^{-1}$ and $\mu_{eff} = 2.8279[(\chi_M)(T - \theta)]^{1/2}$.

$Mn(CO)_5Yb(Me_5C_5)_2 \cdot {}^1/_4PhMe$. Bis(pentamethylcyclopentadienyl)ytterbium–diethyl ester (1.0 g, 0.0019 mol) in toluene (50 mL) was added to decacarbonyldimanganese (0.38 g, 0.00097 mol) in toluene (20 mL). The dark blue solution was stirred for 12 h and filtered, and the filtrate was concentrated to ca. 40 mL. Cooling to −10 °C yielded dark blue prisms, which were collected and dried

(17) Tilley, T. D.; Andersen, R. A.; Spencer, B.; Zalkin, A. *Inorg. Chem.* **1982**, *21*, 2647.

(18) (a) Frenz, B. A.; Ibers, J. A. *Inorg. Chem.* **1972**, *11*, 1109. (b) Clegg, W.; Wheatley, P. J. *J. Chem. Soc. A* **1971**, 3572; *J. Chem. Soc., Dalton Trans.* **1973**, 90; **1974**, *424*, 511. (c) Katacher, M. L.; Simon, G. L. *Inorg. Chem.* **1972**, *11*, 1651. (d) Herberhold, M.; Wehrmann, F.; Neugebauer, D.; Huttner, G. *J. Organomet. Chem.* **1978**, *152*, 329.

under reduced pressure. A second crop of blue prisms was isolated from the mother liquor. The combined yield was 1.0 g (82%). When heated in a sealed capillary, the compound darkened at ca. 270 °C and decomposed at ca. 320 °C. Anal. Calcd for $C_{25}H_{30}MnO_5Yb \cdot {}^1/_4PhMe$: C, 48.6; H, 4.88. Found: C, 48.6; H, 4.70. ^1H NMR: δ 8.75 ($\nu_{1/2}$ = 47 Hz, 30 H), 2.11 (0.75 H); aromatic hydrogens of toluene of solvation obscured by residual benzene in benzene-d_6 solvent. IR: 2735 w, 1965 b, s, 1937 sh, 1928 sh, 1882 m, 1840 s, 1775 b, s, 1062 w, 1024 m, 800 w, 735 m, 728 m, 695 sh, 682 s, 669 s, 650 m, 645 m, 592 w, 555 s, 500 m, 463 m, 425 m, 395 m, 325 s, 285 w cm^{-1}. A sample of the complex was dissolved in benzene-d_6 and hydrolyzed with D_2O. Examination of an aliquot of the benzene layer by ^1H NMR spectroscopy showed resonances due to Me_5C_5D and PhMe in area ratio 8:1.

$Re(CO)_5Yb(Me_5C_5)_2 \cdot {}^1/_4PhMe$. Bis(pentamethylcyclopentadienyl)ytterbium–diethyl ether (0.21 g, 0.00040 mol) in toluene (25 mL) was added to decacarbonyldirhenium (0.13 g, 0.00020 mol) in toluene (10 mL), and the solution was stirred for 48 h. The dark red solution was filtered, and the filtrate was concentrated to ca. 5 mL and cooled (−10 °C). The red microcrystals were collected and dried under reduced pressure: yield 0.17 g (53%); mp 315–320 °C dec. Anal. Calcd for $C_{25}H_{30}O_5ReYb \cdot {}^1/_4C_7H_8$: C, 40.5; H, 4.07. Found: C, 40.4; H, 4.18. ^1H NMR: δ 9.56 ($\nu_{1/2}$ = 110 Hz, 30 H), 2.10 (0.75 H); aromatic protons of solvated toluene obscured by residual benzene in benzene-d_6 solvent. A sample of the complex in benzene-d_6 was hydrolyzed with D_2O. Examination of the benzene solution by ^1H NMR spectroscopy showed resonances due to Me_5C_5D and PhMe in area ratio 8:1. IR: 2720 w, 1982 sh, 1972 s, 1950 s, 1945 sh, 1750 b, s, 1015 w, 950 m, 795 m, 715 m, 625 w, 585 s cm^{-1}.

X-ray Crystallography. Crystals suitable for an X-ray study were grown from toluene and inserted into a quartz capillary, which was then flame sealed. Preliminary precession photographs indicated that the cell dimensions were large and suggested a monoclinic Laue symmetry. The derived cell dimensions were a = 18.0 Å, b = 16.2 Å, c = 18.9 Å, and β = 80° with V = 5450 Å^3. The crystal used for data collection was mounted on an Enraf-Nonius CAD4 automated diffractometer[19] and centered in the beam. A first-peak search followed by automatic indexing gave a near-monoclinic cell with a = 9.44 Å, b = 16.3 Å, c = 18.1 Å, β = 80°, and V = 2750Å^3. Location of additional peaks followed by automatic indexing gave a triclinic primitive cell with a volume of 5500 Å^3, the same as found in the primitive monoclinic cell from the precession work. Inspection of the Niggli values[20] for this cell indicated that there were no cells of higher symmetry; the symmetry derived from the precession photographs was dismissed as "pseudosymmetry". Accurate cell dimensions were obtained by centering the high-angle reflections, and collection of a hemisphere of data was started (Table V).

After transfer and reduction of the first half of the data, certain symmetries were noted in the Patterson and E maps, and a Delaunay reduction was performed on the cell. The program TRACER[21] immediately discovered the C-centered monoclinic unit cell, which was confirmed by reduction and refinement of the data. The crystal parameters in Table V are for this monoclinic cell.

The 14401 raw intensity data were reduced to structure factor amplitudes with their esd's and corrected for scan speed, background, and Lorentz and polarization effects. Analysis of the intensity check reflections showed a nearly linear and highly anisotropic decline in intensity over the data collection period (12 days). The relative intensities of three reflections at the end of the data collection period were 0.94, 0.82, and 0.78 for $\bar{4}$,18,3, 10,14,$\bar{2}$, and 2,4,10, respectively. An anisotropic, linear decay correction was applied to the data, and then the data were transformed to correspond to the monoclinic cell. Inspection of the $h0l$ data showed no systematic absences apart from those generated by the centering operation, giving the choice of space group as $C2$, Cm, or $C2/m$. The latter was confirmed by solution and refinement of the structure. Data were corrected for absorption by an empirical method based upon the observed intensities of the azimuthal-scan data. The maximum and minimum relative transmission factors were 1.00 and 0.919. Averaging of redundant and symmetry-equivalent data yielded 7442 unique reflections; $R(I_{av})$ = 2.3% and $R(F_{av})$ = 1.7%.[22]

Attempts to solve the structure were hampered by the strong pseudotranslation of ${}^1/_2a$. The positions of the metal atoms were finally determined by a combination of vector analysis (Patterson map), direct methods (MULTAN 79), least-squares, and Fourier maps with different numbers and arrangements of atoms in different space groups. The discovery and refinement of the remainder of the atoms, including the toluene of solvation, proceeded by normal least-squares and Fourier techniques. Given the large thermal motion of most of the methyl carbon atoms and the disorder of the toluene, no attempt was made to locate and refine the hydrogen atoms. The R value for all 7442 data (including unobserved reflections) was 4.71%.

Acknowledgment. This work is supported by the Director, Office of Energy Research, Office of Basic Energy Sciences, Chemical Sciences Division of the U.S. Department of Energy, under Contract DE-AC03-76SF00098. We thank Dr. F. J. Hollander, staff crystallographer of the UC X-ray facility (CHEXRAY), for doing the crystal structure, Dr. E. Gamp for his help with the magnetic susceptibility measurements, and the NSF for departmental grants that were used to purchase the X-ray and magnetic susceptibility instruments.

Registry No. $Mn(CO)_5Yb(Me_5C_5)_2$, 88211-39-6; $Mn(CO)_5Yb(Me_5C_5)_2 \cdot {}^1/_4PhMe$, 88211-43-2; $Re(CO)_5Yb(Me_5C_5)_2$, 88211-40-9; $Co(CO)_4Yb(Me_5C_5)_2(thf)$, 88211-42-1; $(Me_5C_5)_2Yb(OEt_2)$, 74282-47-6; $Mn_2(CO)_{10}$, 10170-69-1; $Re_2(CO)_{10}$, 14285-68-8.

Supplementary Material Available: Listings of thermal parameters, carbon–carbon bond lengths, and structure factors (35 pages). Ordering information is given on any current masthead page.

(19) Instrumentation at the University of California Chemistry Department X-Ray Crystallographic Facility (CHEXRAY) consists of two Enraf-Nonius CAD-4 diffractometers, one controlled by a DEC PDP 8a with a RK05 disk and the other by a DEC PDP 8e with a RL01 disk. Both diffractometers use Enraf-Nonius software as described in: "Cad-4 Operation Manual"; Enraf-Nonius: Delft, Holland, Nov 1977; updated version, Jan 1980.

(20) Roof, R. B. "A Theoretical Extension of the Reduced-Cell Concept in Crystallography", Publication LA-4038; Los Alamos Scientific Laboratory: Los Alamos, NM, 1969.

(21) (a) All calculations were performed on a PDP 11/60 equipped with 128 kilowords of memory, twin RK06 28 MByte disk drives, Versatic printer–plotter, and TU10 tape drive using locally modified Nonius SDP software operating under RSX-11M.[21b] (b) "Structure Determination Package Users' Guide"; Molecular Structure Corp.: College Station, TX, April 1980.

(22) $R(x_{av}) = \sum_i ||\bar{x}| - |x_i|| [\sum_i x_i]^{-1}$.